2009 American WJTA Conference and Expo
August 18-20, 2009 ● Houston, Texas

Paper

AWIJ CUTTING OF STRUCTURES MADE OF MAGNESIUM ALLOYS FOR THE CARDIOVASCULAR SURGERY

C. Biskup, M. Hepke, N. Grittner, T. Plorin, T. Hassel, D. Bormann, Fr.-W. Bach
Institute of Materials Science
Leibniz Universität Hannover
Garbsen, Germany

T. Schilling, A. Hilfiker, S. Cebotari, I. Tudorache, T. Meyer, A. Haverich
Leibniz Research Laboratories for Biotechnology and Artificial Organs (LEBAO)
Hannover Medical School
Hanover, Germany

ABSTRACT

Cardiovascular diseases are the most frequent cause for morbidity and mortality worldwide. The damage of the heart muscle's tissue is irreversible since cardiomyocytes do not have the capability to divide, and therefore myocardial regeneration does not take place. A surgical approach for therapy is the substitution of damaged heart tissue by a decellularized and revascularized small intestine mucosa. For the right ventricle and the atria (pressures $\leq$ 40-60 mmHg) the substitution of the damaged area could already be realized in animal studies. However, for the left ventricle (pressures up to 240 mmHg) the mechanical strength of these myocardial grafts is not sufficient in the early stage after the surgery.

In this work first results in the processing of stabilising structures made of magnesium alloys for the cardiovascular surgery by high precision AWIJ are presented. In detail the aspects of cutting strategy, geometrical design, cutting edge roughness and burr generation are discussed.

Organized and Sponsored by the WaterJet Technology Association

1. INTRODUCTION

Various patch materials currently used for cardiac reconstruction represent a non-viable tissue with high susceptibility to infection and degeneration and without the ability to remodel or to grow with the host. We introduce an innovative autologous vascularized matrix (AutoVaM) with high regenerative potential for myocardial reconstruction based on a segment of stomach including its vessels. Autologous stomach segments without mucosa but with adjacent gastric artery and vein were used for the replacement of right ventricular transmural defects in pigs in a chronic animal study. The autografts were revascularized by connecting gastric vessels to the right internal thoracic artery and vein. We showed feasibility to use these grafts as patch material for the right heart [1]. An autologous vascularized matrix has successfully been used twice to repair a severe myocardial lesion of the right atrium in human patients as a last resort in these cases. Nevertheless its applicability in the left heart cannot be recommended yet: The stability of AutoVaM in the high pressure system is not sufficient in the early stage after surgery following risk of rupture. Moreover paradox movements of the repaired segment leading to low ejection fraction avoid its clinical use.

Hence there is a strong need to support the biological patch material to achieve mechanical durability until remodelling of the gastric tissue stabilises the graft. On this purpose we developed scaffolds of magnesium alloys to be externally fixed to the initially fragile patch.

2. STABILISING STRUCTURES

2.1 Biodegradable magnesium alloys

For the experiments magnesium alloys with different compositions were melted in a controlled atmosphere furnace. The choice of alloys was geared to preliminary tests regarding the biocompatibility of different magnesium alloys [2-5]. Hence, the following study is based on available data relating to the resorption kinetic as well as the biological compatibility. The special requirements for the used alloys are a high ductility and fatigue strength. Therefore beside the standard forgeable alloy AZ31 two modified alloys with different lithium concentrations (LA33, LA63) were selected for the study.

2.2 Requirements

The task of the structures is the stabilization of the AutoVaM for a certain time. Therefore the design of the structures has to be planar with a maximal contact area between structure and AutoVaM. The diameter of the structures depends on the heart defect which shall be reconstructed. Structures of 30 to 60 mm in diameter seem to be sufficient. However, the heart movement must not respectively only minimally be constrained by the structure. Thus there must be an adequate elasticity in the radial and orthogonal direction of the structure. Of course the stabilizing structures must have a sufficient fatigue resistance in the biological environment as well. But the main point that has to be fulfilled by the structure is that there is no risk of AutoVaM damage. For this reason it is crucial for the manufacturing to avoid sharp edges.

2.3 Design

Different geometries were designed and checked if the requirements were fulfilled (see Figure 1). Structures 1 to 5 do not fulfil the requirement of elasticity in the radial direction. Only structures 6 to 9 were capable to move in the radial direction by the use of a meander shape. The elasticity in orthogonal direction depends on the thickness of the structure. Thicknesses of 0.5 mm seem to be adequate for the application.

2.4 Cutting strategy

A cutting strategy with 4 steps was developed to cut small structures with bar widths of 1 mm (see Figure 2a). In the first step the bores were drilled in the material. In step two only the half of the structure was cut. Preliminary tests showed that the structure bends in the axial direction when cutting the whole structure at once. For this reason the structure could not be cut without damaging the small bars. Therefore after step two a thin steel sheet with a thickness of 0.2 mm was placed beneath the material to reinforce the structure for cutting the second half of the structure. In an fourth step the structure was separated from the material sheet. Different structures could be manufactured using this strategy (see Figure 2b).

2.5 Necessity of further investigations

For AWIJ cutting of the stabilizing structures with small bar widths in thin sheets the influence of the AWIJs' parameters on the width of cut are crucial to reach precise geometries. Moreover burr generation took place during our tests, which has to be quantified and minimized because of the risk of damaging the AutoVaM. The roughness of the cutting edges could be an important factor to control the structures' corrosion respectively the biodegradation in the body environment. In the following results of a study regarding the width of cut, the maximum burr height and the roughness in dependence of the AWIJ's parameters and different materials are presented.

3. MATERIAL AND METHODS

3.1 Sheet production of magnesium alloys

The casted magnesium alloys were turned to cylinders with a diameter of 120 mm and a length of 300 mm and a solution heat treatment were applied. Afterwards the heated blocs were extruded by a 10 MN extrusion press (SMS Meer) to sheets of 0.5 mm in thickness and a width of 61 mm.

3.2 Experimental set up

For the experiments a high pressure intensifier (Böhler, Typ DU 400-4 / PL) with a maximal pressure of 400 MPa and a maximal flow rate of 4 l/min was used. The cutting table consisted of a catcher, a controlled X/Y axis and a Z axis, which can be manipulated manually. The machine, the valves and the abrasive dosing system were numerical controlled by a Berger Lahr NC-control system. An orifice diameter of 0.17 mm and a focusing tube diameter of 0.6 mm were used for all experiments. Sheets of 0.5 mm thickness were used for the experiments. For the tests the sheets were clamped on 5 mm thick wood plates and straight cuts were performed with a length of 20 mm and different sets of parameters. The parameters which were varied are target material, abrasive material, abrasive particle size distribution, abrasive mass flow rate, pressure, traverse rate and standoff distance.

3.3 Measurement technique

The burr height and the width of cut were measured by a 3D-Laser Scanning Microscope (Keyence VK9700). The solution in z-direction was set to 0.2 µm. The 3D-data were evaluated by the software VK-Analyser (see Figure 3). The maximal burr height was measured at the bottom side of the specimen at five different positions and the average was taken.

The roughness was measured by a laser optical topography measurement system (Rodenstock RM 600) at the middle of the cutting edges. The focus diameter of the laser was 1 µm with a vertical resolution of 0.3 µm. The mean roughness R_a was chosen to compare the influence of parameters on the surface roughness of the cuts.

4. RESULTS

4.1 Burr generation and width of cut

The generation of burrs strongly depends on the target material which is cut by the AWIJ. Figure 4 shows the results of the maximum burr height for different materials like iron, stainless steel, brass and different magnesium alloys (AX30, LA33, LA63 and AZ31). The burr height increases with an increase in material ductility. Anyway it was found that the width of cut behaves in the opposite way (see Figure 5).

The comparison of abrasive material showed no significant differences between GMA Garnet and Barton Garnet. However the maximum burr height can be significantly reduced by using smaller abrasive particles. With #200 (GMA Garnet) respectively #220 (Barton Garnet) the maximum burr heights could be reduced about 33% in comparison to #80 (see Figure 6).

In Figure 7 the pressure was varied in the range of 50 to 300 MPa. Although the cutting performance of 50 MPa was sufficient to cut the sheets with parallel cutting edges a decrease of the maximal burr height with an increase of pressure was detected. For low pressures of 50 MPa burr heights of more than 230 µm could be measured. For a pressure higher than 200 MPa the burr height oscillated around 100 µm. The width of cut rises nearly linearly with the pressure from values below the focusing tube diameter of 0.6 mm to 0.7 mm.

The burr generation in thin sheets is very sensitive to the standoff distance. The maximal burr height doubles its values from app. 100 µm to 200 µm for a change of standoff distance from 1 mm to 5 mm. Because of the jet's divergence the width of cut increases significantly with a rise in standoff distance. Standoff distances until 2 mm have no large influence on the width of cut (Figure 8).

An optimal abrasive mass flow rate exists at which the burr height reaches a minimal value. The maximum burr height could be nearly halved by using 4 g/s instead of 1 g/s. The cutting width increases negligible about 5 % by using an abrasive mass flow rate of 6 g/s instead of 1 g/s (see Figure 9).

4.2 Roughness

Figure 11 shows the mean roughness against the abrasive mass flow rate. It can be concluded that the higher the abrasive mass flow rate the smaller the mean roughness. Anyway, no optimal mass flow rate could be identified regarding the mean roughness.

Furthermore it can be seen that for higher traverse rates the mean roughness increases. This tendency can be verified with results shown in Figure 12, where the mean roughness is shown in dependence of the traverse rate for different particle size distributions. The influence of traverse rate on the mean roughness seems to be higher for coarse abrasive (#80) than for small particles (#220).

5. SUMMARY AND CONCLUSIONS

In this study stabilising, biodegradable structures for the cardiovascular surgery were introduced. The function of these structures is the stabilisation of a biological implant for a certain time. Structures with a meander shape fulfil the requirement of elasticity in radial direction. A necessary elasticity in orthogonal direction was achieved by a small thickness of the structures of 0.5 mm.

To avoid burr generation which could damage the thin biological prostheses, studies were performed to investigate the AWIJ's parameters influence on the maximum burr height by cutting thin sheets of different materials.

On the one hand the maximum burr height could be significant reduced by using lower traverse rates and higher pressures as described in previous studies [6, 7]. On the other hand the enhancement of these parameters results in bigger width of cuts, which has to be taken into account for the path correction of small structures.

The usage of small abrasive particles is recommended to reduce the burr height. No positive influence could be detected by using the sharp edged Barton Garnet instead of natural GMA Garnet, which could be explained by the fragmentation of the abrasive during the acceleration process in the mixing tube. An optimum abrasive mass flow rate could be identified at 4 g/s for the used AWIJ's settings, at which the burr height reaches its minimum. Because the width of cut only changes negligible with the increase of abrasive mass flow rate, it seems to be an adequate method to reduce burr formation.

The standoff distance should be chosen smaller than 2 mm to minimize the burr formation and to achieve small cutting widths.

The surface roughness is influenced by the traverse rate and the abrasive mass flow rate significantly. The more particles contribute to the removal process the smaller the mean roughness R_a. The effect is more distinct for larger particles.

6. ACKNOWLEDGEMENT

The authors are members of the Waterjet Laboratory Hannover (WLH) and of the German Working Group of Waterjet Technology (AWT).

The results presented here were acquired within the framework of the collaborative research centre 599 financed by the German Research Foundation (DFG). The authors would like to thank the DFG for their support.

7. REFERENCES

[1] Haverich, A; Lichtenberg, A.; Cebotari, S.; Tudorache, I.: Bioartificial heart tissue graft and method for the production thereof. Patent WO2006/122533 A2, 2006

[2] Höh von der, N.; Bormann, D.; Lucas, A.; Denkena, B.; Hackenbroich, C.; Meyer-Lindenberg, A.: Influence of different surface machining treatments of magnesium-based implants on the degradation behaviour on rabbits; Afvances Engineering Materials 2009, 11, No. 5; pp. 47-54

[3] Höh von der N., Rechenberg von B., Bormann D., Lucas A., Meyer-Lindenberg A.: Influence of different surface machining treatments of resor-bable magnesium alloy implants on degradation - EDX-analysis and histolo-gical results; Biomaterials NRW - Fundamentals and Clinical Applications (2008) 48-49

[4] Krause Ch., Bach Fr.-W., Bormann D., Zeddies M., Krause A., Meyer-Lindenberg A., Windhagen H.: Resorbierbare Marknägel auf Magnesiumba-sis; Schweizer Maschinenmarkt 01/02 (2008) pp. 94-99

[5] Krause Chr., Bormann D., Hassel Th., Bach Fr.-W., Windhagen H., Krause A., Chackenbroich Chr., Meyer-Lindenberg A.: Mechanical Properties of De-gradable Magnesium Implants in Dependance of the Implantation Duration; Magnesium Technology in the Global Age, 45th Annual Conference of Met-allurgists of CIM, Montreal, Quebec, Canada (2006) pp. 329-343

[6] Gropetti, R., Gutema, T., and Di Lucchio, A.: A contribution to the analysis of some kerf quality attributes for precision abrasive waterjet cutting. 14th International Conference on Jetting Technology. (1992), Bury St. Edmunds [u.a.], Professional Engineering Publishing, 253/272

[7] Hashish, M.: Characteristics of surfaces machined with abrasive-waterjet. Journal of Engineering Materials and Technology, Vol. 113, 1991, pp 354-362

8. FIGURES

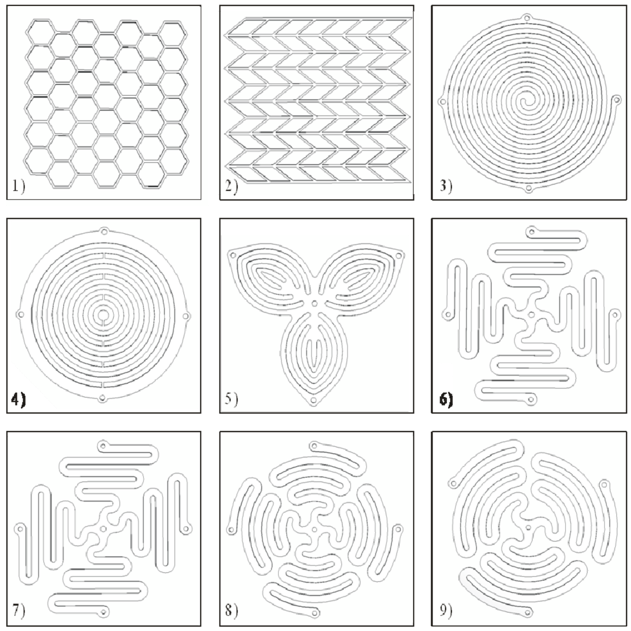

Figure 1. Different designs of possible stabilizing structures

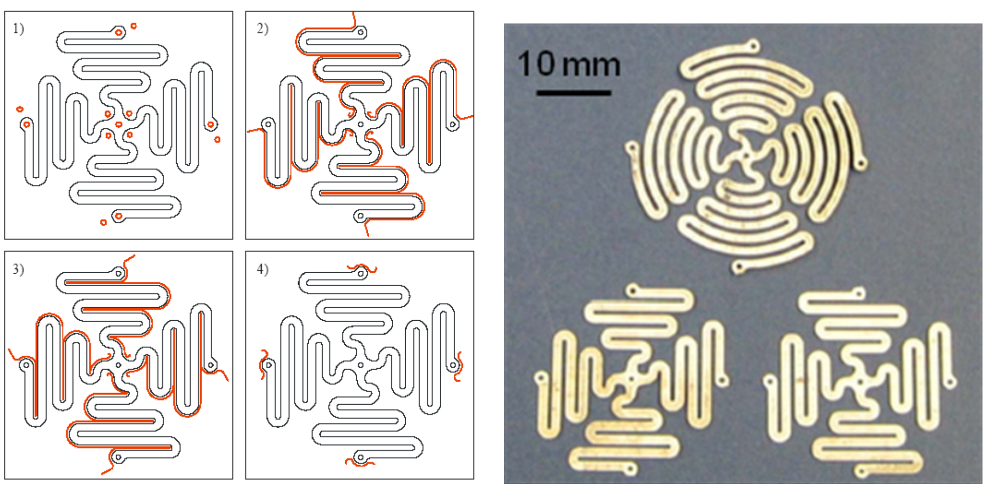

Figure 2. Cutting strategy to cut stabilising structures (left);
Different manufactured stabilising structures (right)

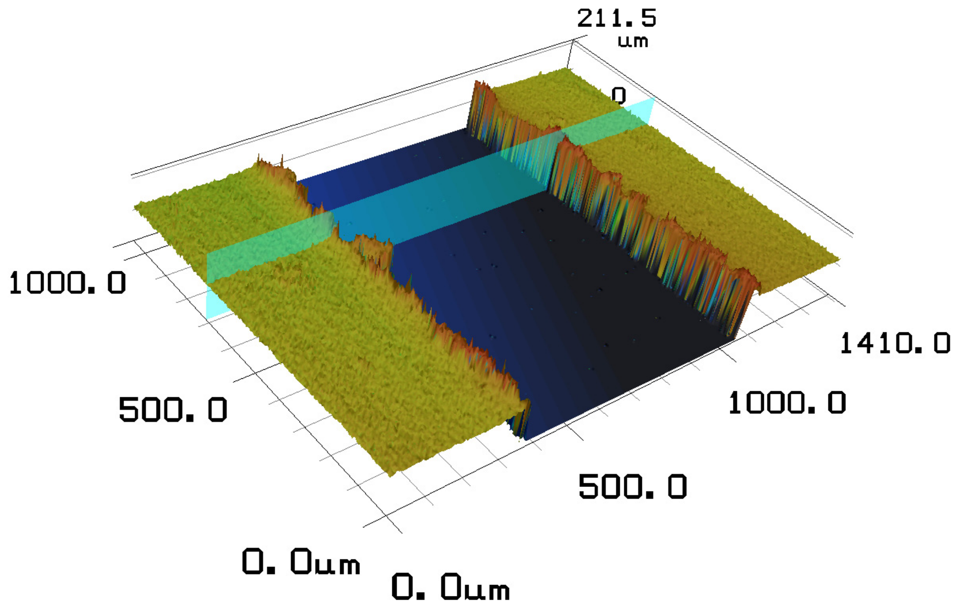

Figure 3. 3D-view of a cut with measurement plane.

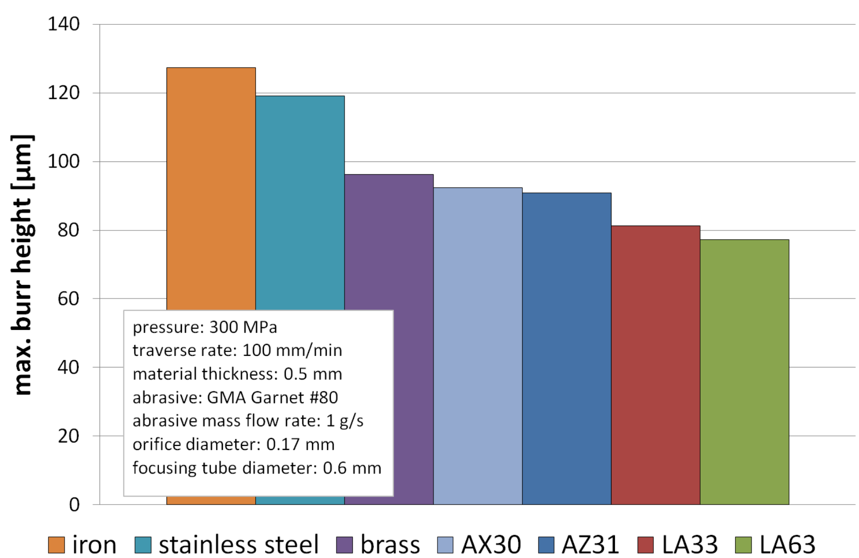

Figure 4. Max burr height in dependence on the target material.

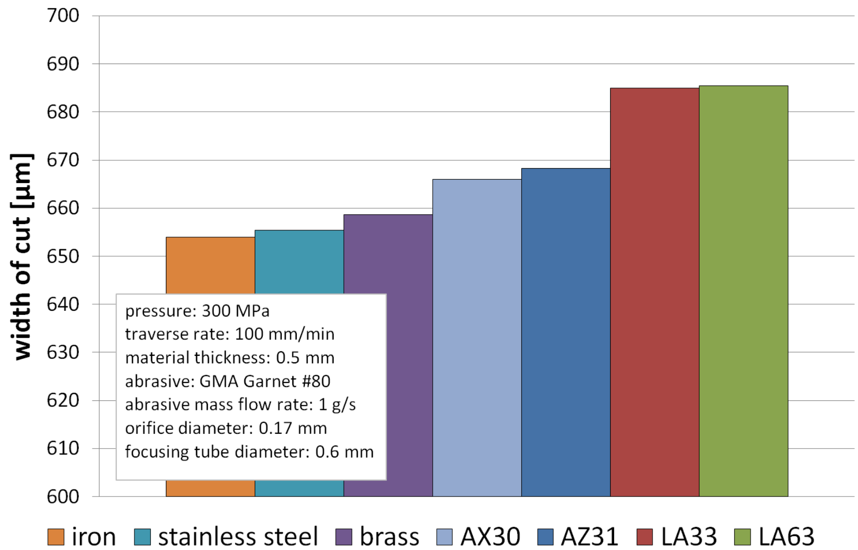

Figure 5. Width of cut in dependence on the target material.

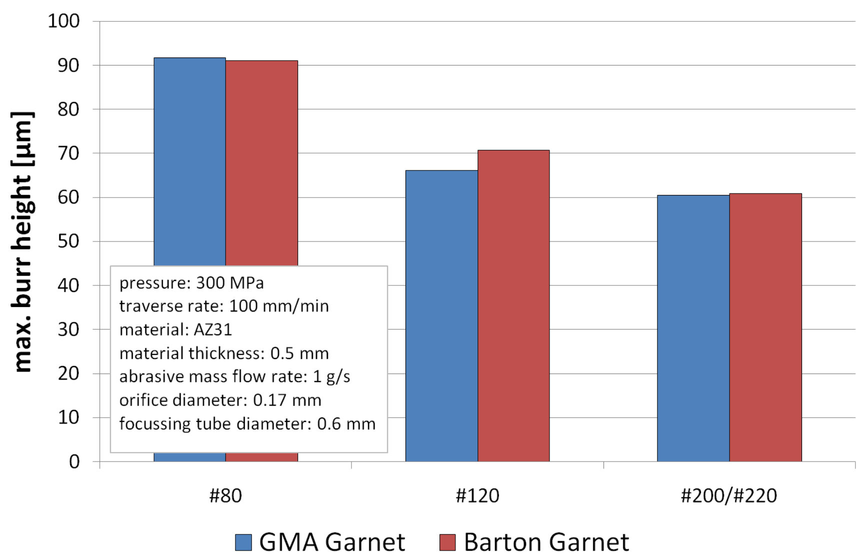

Figure 6. Max. burr height in dependence of the abrasive material and abrasive particle size

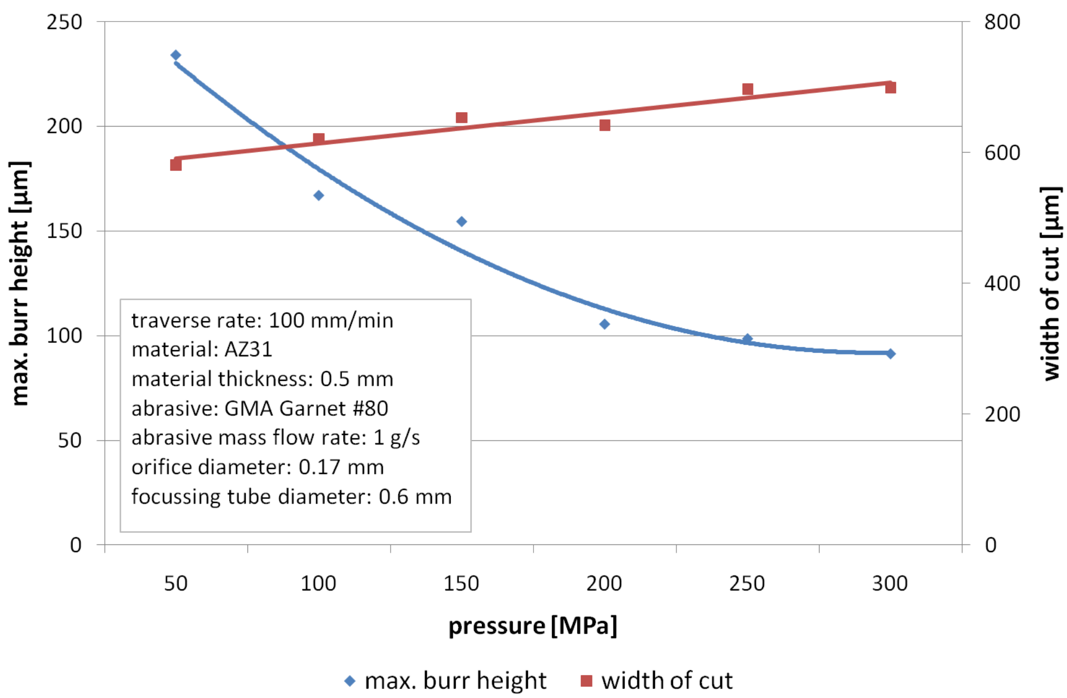

Figure 7. Max. burr height in dependence on the pump pressure

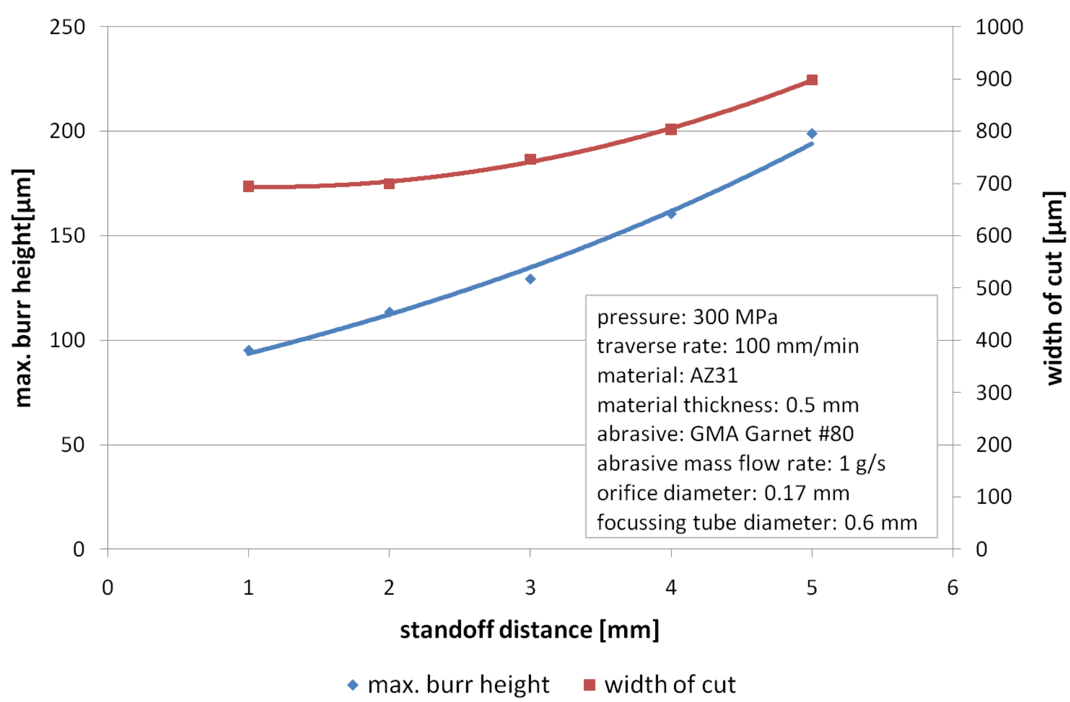

Figure 8. Max. burr height and width of cut in dependence of the standoff distance

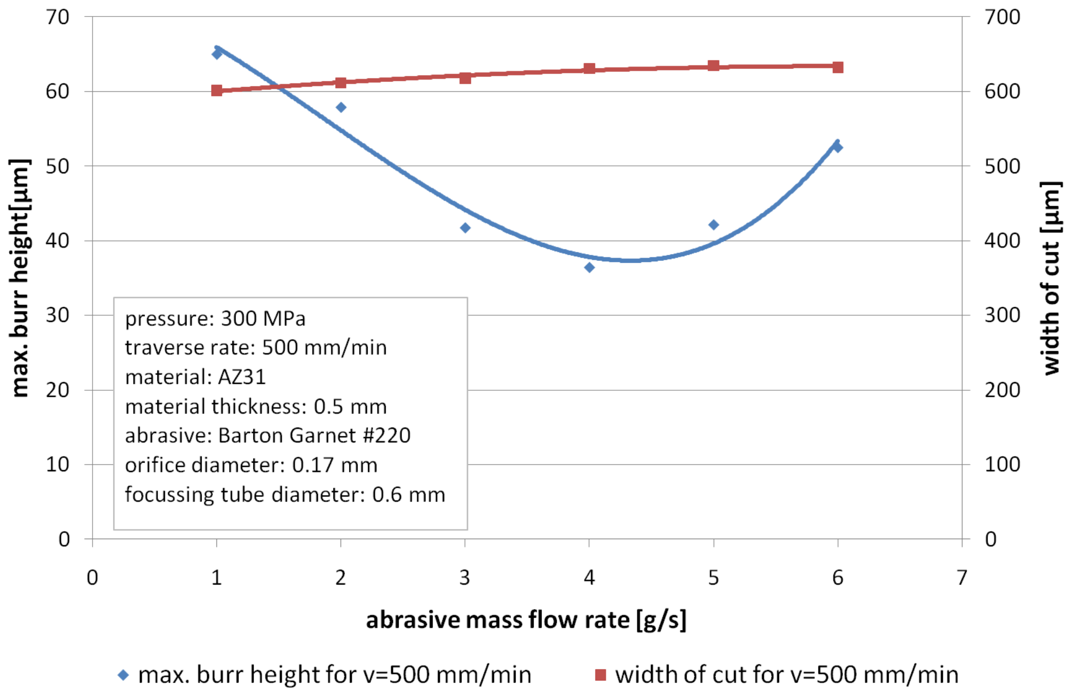

Figure 9. Max. burr height and width of cut in dependence of the abrasive mass flow rate

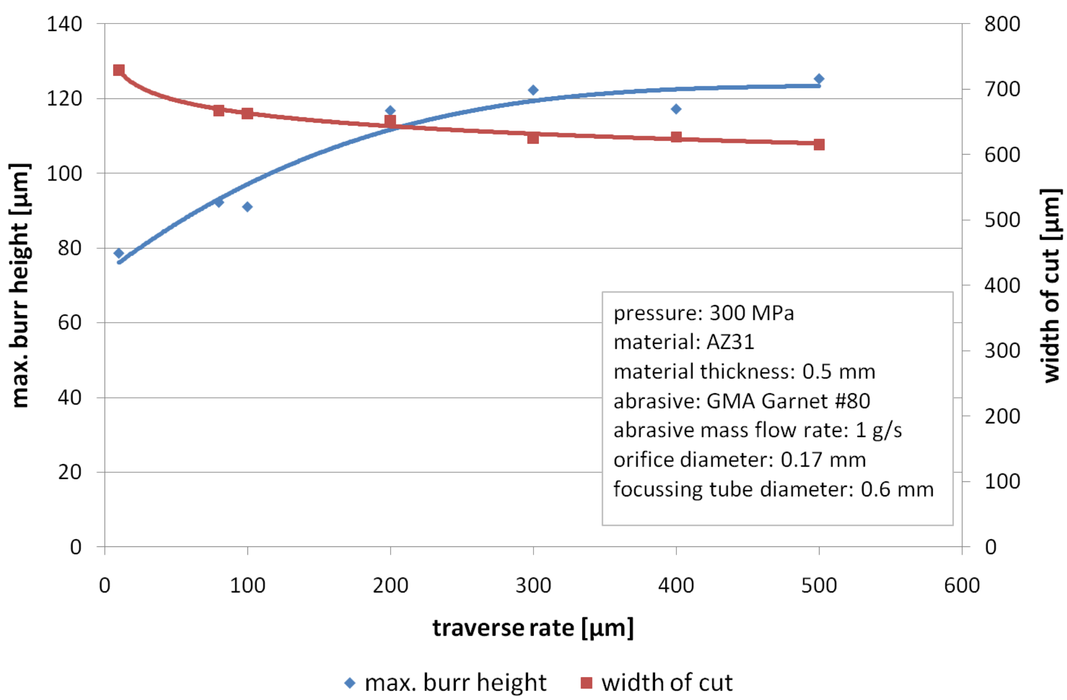

Figure 10. Max. burr height and width of cut in dependence of the traverse rate

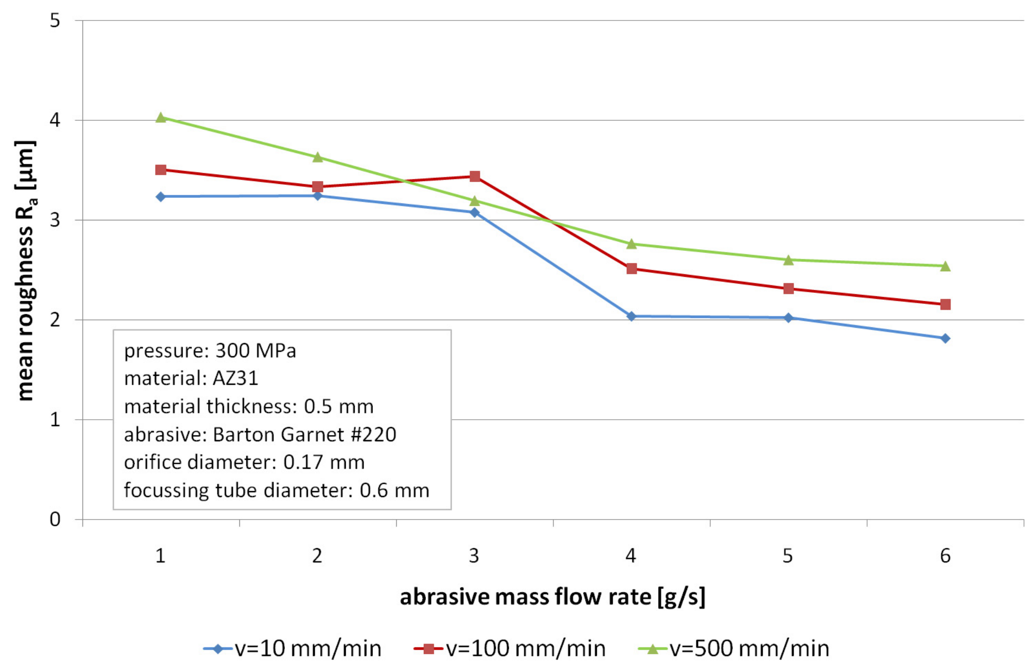

Figure 11: Mean roughness in dependence on the abrasive mass flow rate for different traverse rates

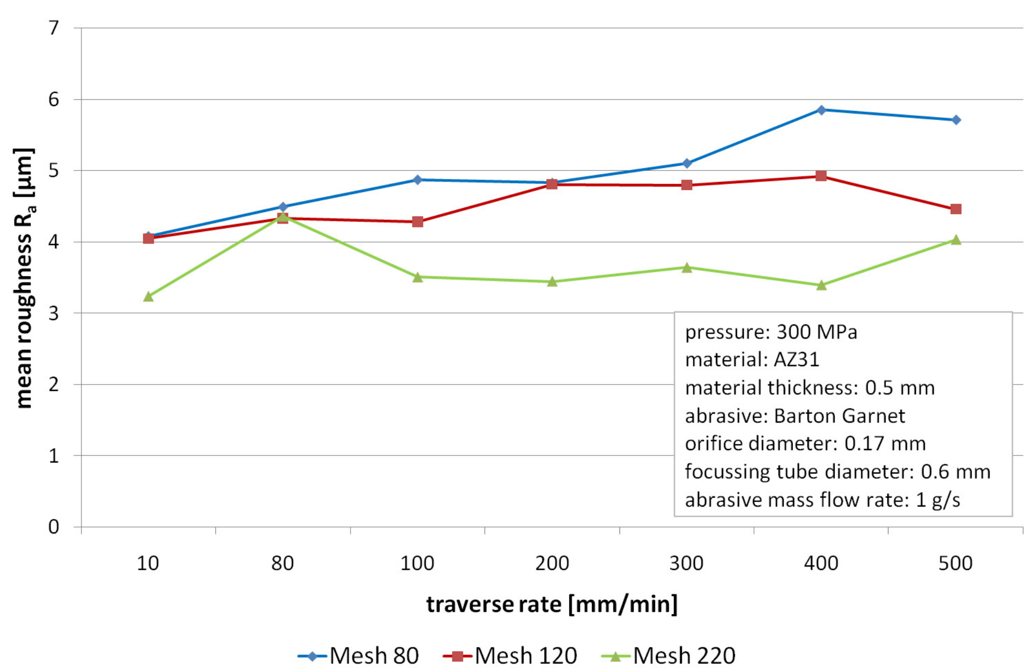

Figure 12: Mean roughness in dependence on the traverse rate for different particle size distributions